

**AFRL-PR-WP-TR-2001-2042**

**THERMAL MANAGEMENT RESEARCH  
STUDIES**

**VOLUME 2: EXPERIMENTAL INVESTIGATION  
OF OSCILLATING HEAT PIPES FOR ACTUATOR  
COOLING**



**LANCHAO LIN, Ph.D.**

**UES, INC.  
4401 DAYTON-XENIA ROAD  
DAYTON, OH 45432-1894**

**MARCH 2001**

**FINAL REPORT FOR PERIOD 20 AUGUST 1996 – 31 DECEMBER 2000**

**Approved for public release; distribution unlimited**

**20010515 021**

**PROPULSION DIRECTORATE  
AIR FORCE RESEARCH LABORATORY  
AIR FORCE MATERIEL COMMAND  
WRIGHT-PATTERSON AIR FORCE BASE, OH 45433-7251**

## NOTICE

USING GOVERNMENT DRAWINGS, SPECIFICATIONS, OR OTHER DATA INCLUDED IN THIS DOCUMENT FOR ANY PURPOSE OTHER THAN GOVERNMENT PROCUREMENT DOES NOT IN ANY WAY OBLIGATE THE US GOVERNMENT. THE FACT THAT THE GOVERNMENT FORMULATED OR SUPPLIED THE DRAWINGS, SPECIFICATIONS, OR OTHER DATA DOES NOT LICENSE THE HOLDER OR ANY OTHER PERSON OR CORPORATION; OR CONVEY ANY RIGHTS OR PERMISSION TO MANUFACTURE, USE, OR SELL ANY PATENTED INVENTION THAT MAY RELATE TO THEM.

THIS REPORT IS RELEASABLE TO THE NATIONAL TECHNICAL INFORMATION SERVICE (NTIS). AT NTIS, IT WILL BE AVAILABLE TO THE GENERAL PUBLIC, INCLUDING FOREIGN NATIONS.

THIS TECHNICAL REPORT HAS BEEN REVIEWED AND IS APPROVED FOR PUBLICATION.



RENGASAMY PONNAPPAN  
Senior Mechanical Engineer  
Energy Storage & Thermal Sciences Branch



BRIAN G. HAGER  
Chief  
Energy Storage & Thermal Sciences Branch



JOE MCNAMEE, Major, USAF  
Deputy Chief  
Power Division

Do not return copies of this report unless contractual obligations or notice on a specific document requires its return.

REPORT DOCUMENTATION PAGE			Form Approved OMB No. 074-0188	
Public reporting burden for this collection of information is estimated to average 1 hour per response, including the time for reviewing instructions, searching existing data sources, gathering and maintaining the data needed, and completing and reviewing this collection of information. Send comments regarding this burden estimate or any other aspect of this collection of information, including suggestions for reducing this burden to Washington Headquarters Services, Directorate for Information Operations and Reports, 1215 Jefferson Davis Highway, Suite 1204, Arlington, VA 22202-4302, and to the Office of Management and Budget, Paperwork Reduction Project (0704-0188), Washington, DC 20503				
1. AGENCY USE ONLY (Leave blank)	2. REPORT DATE March 2001	3. REPORT TYPE AND DATES COVERED Final, 08/20/1996 - 12/31/2000		
4. TITLE AND SUBTITLE  Thermal Management Research Studies Volume 2: Experimental Investigation of Oscillating Heat Pipes for Actuator Cooling		5. FUNDING NUMBERS C: F33615-96-C-2680 PE: 62203F PN: 3145 TN: 20 WU: C4		
6. AUTHOR(S) Lanchao Lin, Ph.D.				
7. PERFORMING ORGANIZATION NAME(S) AND ADDRESS(ES)  UES, INC. 4401 DAYTON-XENIA ROAD DAYTON, OH 45432-1894		8. PERFORMING ORGANIZATION REPORT NUMBER  UES-P155-01-001 (Vol. 2)		
9. SPONSORING / MONITORING AGENCY NAME(S) AND ADDRESS(ES)  PROPULSION DIRECTORATE AIR FORCE RESEARCH LABORATORY AIR FORCE MATERIEL COMMAND WRIGHT-PATTERSON AIR FORCE BASE, OH 45433-7251 POC: RENGASAMY PONNAPPAN, AFRL/PRPS, (937) 255-2922		10. SPONSORING / MONITORING AGENCY REPORT NUMBER  AFRL-PR-WP-TR-2001-2042		
11. SUPPLEMENTARY NOTES: The other volume of this report is: Thermal Management Research Studies Volume 1: High Performance Miniature Heat Pipes. (AFRL-PR-WP-TR-2001-2041)				
12a. DISTRIBUTION / AVAILABILITY STATEMENT Approved for public release; distribution unlimited.			12b. DISTRIBUTION CODE	
13. ABSTRACT (Maximum 200 Words)  Operation requirements of oscillating heat pipes (OHPs) were proposed. Based on the requirements, OHPs with acetone and nonflammable fluorocarbon fluids, FC-72 and FC-75, as the working fluid were developed. The OHPs had 40 tubing turns formed from a copper tubing with an inner diameter of 1.75 mm and a total length of 18.61 m. The OHPs were formed in the shape of a planer array that was 256-mm wide and 446-mm high. There were two condensers on both outer sides and one evaporator in the middle of the OHPs. Thermal performance tests were conducted at various operating temperatures and heat rates. The working fluid fill ratio was varied. The OHPs with acetone and FC-72 exhibited their highest heat transport performance in excess of 2000 W without dryout. This is the first time that such a performance was demonstrated. The gravitational acceleration did not have noticeable influence on the performance of the OHPs. The thermal performances of the fluorocarbon OHPs were compared with the case of the acetone OHP.				
14. SUBJECT TERMS Actuator cooling, oscillating heat pipe, two-phase flow, flow instability, slug flow, evaporator heat transfer coefficient, condenser heat transfer coefficient, minimum tubing turn number			15. NUMBER OF PAGES 46	
			16. PRICE CODE	
17. SECURITY CLASSIFICATION OF REPORT Unclassified	18. SECURITY CLASSIFICATION OF THIS PAGE Unclassified	19. SECURITY CLASSIFICATION OF ABSTRACT Unclassified	20. LIMITATION OF ABSTRACT SAR	
NSN 7540-01-280-5500		Standard Form 298 (Rev. 2-89) Prescribed by ANSI Std. Z39-18 298-102		

## TABLE OF CONTENTS

	Page
LIST OF FIGURES	iv
NOMENCLATURE	vi
LIST OF APPLICABLE DOCUMENTS	viii
FOREWORD	ix
1 INTRODUCTION	1
2 REQUIREMENTS OF OPERATION	3
3 EXPERIMENTAL SETUP AND PROCEDURE	5
4 MEASUREMENT UNCERTAINTY	12
5 RESULTS AND DISCUSSION	13
5.1 Results of Acetone Heat Pipe	13
5.2 Results of Fluorocarbon Heat Pipes	20
5.3 Comparison of OHPS with Different Working Fluids	26
6 CONCLUSIONS AND RECOMMENDATIONS	27
6.1 Conclusions	27
6.2 Recommendations	28
7 REFERENCES	29
APPENDIX A ASSEMBLY DRAWING OF OHP TEST RIG	30

## LIST OF FIGURES

Figure	Page
3.1 OHP and thermocouple locations.	6
3.2 Photographic view of the OHP.	6
3.3 Schematic of OHP experimental setup.	8
3.4 Thermal conduction plate.	9
5.1 Comparison between the heat rate through the top condenser ( $Q_1$ ) and bottom condenser ( $Q_2$ ).	14
5.2 Heat transfer coefficients vs. total heat rate for $T_{m3} = 55^\circ\text{C}$ and $\phi=50\%$ in vertical position.	15
5.3 Heat transfer coefficients vs. total heat rate for $T_{m3} = 55^\circ\text{C}$ and $\phi=50\%$ in horizontal position.	16
5.4 Heat transfer coefficients vs. total heat rate for $\phi=50\%$ and $\phi=38\%$ at $T_{m3} = 55^\circ\text{C}$ in vertical position.	17
5.5 OHP wall temperature profiles along the middle tube of the OHP at different total heat rates for $T_{m3} = 55^\circ\text{C}$ and $\phi=38\%$ in vertical operation.	18
5.6 OHP wall temperature profiles along the middle tube of the OHP at different total heat rates for $T_{m3} = 55^\circ\text{C}$ and $\phi=32\%$ in vertical operation.	18
5.7 Heat transfer coefficients of the upper evaporator and condenser vs. operating temperature.	19
5.8 OHP wall temperature profiles along the middle tube of the FC-72 OHP at different total heat rates for $T_{m3} = 75^\circ\text{C}$ and $\phi=50\%$ in vertical operation.	20
5.9 Heat transfer coefficients of the evaporator and condenser vs. total heat rate for FC-72 OHP with 50% fill ratio at $75^\circ\text{C}$ operating temperature.	21
5.10 Heat transfer coefficients of the evaporator and condenser vs. total heat rate for FC-75 OHP in vertical operation at $75^\circ\text{C}$ operating temperature.	22
5.11 Excursion of temperatures on the FC-75 OHP with 38% fill ratio during dryout.	23

5.12	Heat transfer coefficients of the upper evaporator and condenser vs. operating temperature.	24
5.13	Comparison between the heat rate through the top condenser ( $Q_1$ ) and bottom condenser ( $Q_2$ ) of the FC-72 and FC-75 OHPs.	25
5.14	Comparison of the heat transfer coefficients of the upper evaporator and condenser in vertical position with those in horizontal position.	25
5.15	Comparison of heat transfer coefficients of the FC-72 OHP with those of FC-75 OHP and acetone OHP with respect to the upper evaporator and condenser.	26

## NOMENCLATURE

- $A$  = outer wall area of tube,  $\text{m}^2$   
 $A_i$  = inner cross-sectional area,  $\text{m}^2$   
 $Bo$  = Bond number,  $d_b \sqrt{g(\rho_l - \rho_g) / \sigma}$   
 $d$  = tube diameter,  $\text{m}$   
 $g$  = gravitational acceleration,  $\text{m s}^{-2}$   
 $h$  = heat transfer coefficient,  $\text{W m}^{-2} \text{K}^{-1}$   
 $h_{fg}$  = latent heat of vaporization,  $\text{J kg}^{-1}$   
 $j_g$  = vapor superficial velocity,  $\text{m s}^{-1}$   
 $j_{g,c}$  = critical vapor superficial velocity,  $\text{m s}^{-1}$   
 $j_g^*$  = dimensionless vapor superficial velocity,  $j_{g,c} \rho_g^{0.5} / [gd_i(\rho_l - \rho_g)]^{0.5}$   
 $n$  = tubing turn number  
 $Q$  = heat rate (total output heat rate),  $\text{W}$   
 $Q_c$  = onset heat rate for co-current two-phase flow,  $\text{W}$   
 $Q_1$  = heat rate through top condenser,  $\text{W}$   
 $Q_2$  = heat rate through bottom condenser,  $\text{W}$   
 $T$  = temperature,  $^{\circ}\text{C}$   
 $T_{m3}$  = operating temperature,  $^{\circ}\text{C}$   
 $\Delta T$  = temperature difference,  $^{\circ}\text{C}$   
 $\rho_l$  = liquid density,  $\text{kg m}^{-3}$   
 $\rho_g$  = vapor density,  $\text{kg m}^{-3}$   
 $\sigma$  = surface tension,  $\text{N m}^{-1}$   
 $\phi$  = fill ratio

### Subscripts

- $a1$  = top adiabatic section  
 $a2$  = bottom adiabatic section  
 $b$  = liquid bridging

c1 = top condenser

c2 = bottom condenser

e = evaporator

e1 = evaporator related to the top

e2 = evaporator related to the bottom

i = inner

min = minimum



## LIST OF APPLICABLE DOCUMENTS

- AD1. Lin, L., Ponnappan, R., and Leland, E. J., "Heat Transfer Characteristics of an Oscillating Heat Pipe," AIAA Paper 2000-2281, 34<sup>th</sup> AIAA Thermophysics Conference, Denver, 2000.
- AD2. Lin, L., Ponnappan, R., and Leland, E. J., "Experimental Investigation of Oscillating Heat Pipes Cooling," accepted by Journal of Thermophysics and Heat Transfer; also AIAA Paper 2000-2948, 35<sup>th</sup> Intersociety Energy Conversion Engineering Conference, Las Vegas, 2000.

## FOREWORD

This final technical report is part of the contract deliverables under the contract F33615-96-C-2680 titled "Thermal Management Research for Power Generation". This contract was sponsored and administered by Propulsion Directorate (PR) of the Air Force Research Laboratory (AFRL), Wright-Patterson Air Force Base. The present report deals with the experimental investigation of oscillating heat pipes. The research effort was performed under Task 002, Actuator Cooling. At various stages of this task, Dr. John E. Leland and Dr. Rengasamy Ponnappan (AFRL) were the Air Force Project Engineers/Technical Monitors.

The work presented here was carried out at the Power Division's Thermal Laboratory by UES, Inc., Dayton, Ohio. The on-site personnel are Dr. Lanchao Lin, Mr. John E. Tennant and Mr. Roger P. Carr (UES, Inc.). Mr. John E. Tennant fabricated oscillating heat pipes and the whole experimental device. Mr. Roger P. Carr helped with the instrumentation and acquired experimental data. UES' Materials and Processes Division and contract office provided the administrative support. The author appreciates the support from Dr. Jerry E. Beam (AFRL) for his encouragement and advice. The author would also like to acknowledge the effort of Mr. Richard J. Harris (UDRI) for designing a high temperature cut out unit and helping with the data acquisition.

## 1 INTRODUCTION

The application of unconventional heat pipes to high power electrically driven actuators, e.g. electromechanical actuators (EMAs), is important since EMAs possess no inherent means of removing heat. The EMA cooling system should have a passive heat transport feature and compact size, be lightweight and respond quickly to actuator duty cycles. To meet these requirements, oscillating heat pipes (OHPs) are selected as the heat transfer element for the cooling system.

The OHP is a closed two-phase heat transfer device consisting of a meandering capillary tube. The OHP uses the oscillation movement of two-phase flow to transport energy from the evaporator to condenser. The OHP operation was experimentally verified for different heat modes relating to OHP orientations<sup>1,2</sup>. Maezawa et al. investigated a chaotic behavior of an OHP with R142b as working fluid by monitoring a tube surface temperature in the adiabatic section. The OHP had a length of 600 mm, an inner diameter of 2 mm and 40 turns. It was confirmed from a chaotic parameter analysis that the temperature oscillation had chaotic characteristics and was governed by the non-periodic dynamic system of two-phase flow<sup>2</sup>. Overall thermal performances of OHP based heat exchangers were presented<sup>2,3</sup>. Kiseev and Zolkin tested an OHP on a spin table<sup>4</sup>. The OHP had an inner diameter of 1.1 mm, a length of 420 mm and 23 turns. Acetone was used as the working fluid and the fill ratio was 60%. It was exhibited that there was an increase of the evaporator temperature by 30% with an increase of the acceleration from an adverse acceleration of  $-6g$  to a favorable acceleration of  $12g$ .

Heat transfer characteristics in the evaporator and condenser of OHPs have not been reported. To obtain the heat transfer coefficients of evaporator and condenser of the OHP and to find the method of enhancing the heat transfer coefficients of the OHP, an experimental investigation of OHPs for the cooling of EMAs has been conducted. The fluorocarbon fluids of FC-72 and FC-75 as well as acetone is used as the working fluid. The fluorocarbon fluids are selected due to their non-flammability feature that is desired for the cooling of aircraft EMAs. Heat pipes with FC-72 and FC-75 as the working fluid have not been reported before. The design of the OHP test setup is aimed at achieving high performances of the OHP in a wide range of the OHP operating temperatures from

25°C to 85°C. The fill ratio of the working fluid is varied to find a suitable fill ratio. The input power is adjusted in the range of 140 W - 2100 W. A comparison of OHP heat transfer characteristics between the vertical operation and horizontal operation is made and the effect of the gravitational acceleration on the thermal performance of OHP is addressed.

## 2 REQUIREMENTS OF OPERATION

An effective operation of the OHP relies on the oscillation movement of the two-phase flow in the OHP. The two-phase flow oscillation, a flow instability, is related to the fact that the pressure drops in each channel between two consecutive turns are not in phase with each other. A basic flow pattern in the OHP can be the slug flow caused by liquid bridging or an oscillating co-current two-phase flow depending on the type of working fluid and the tube diameter. The performance limitation of the OHP is caused by dryout due to an insufficient liquid supply to the evaporator.

The slug flow (liquid bridging) occurs under the condition that the inner tube diameter of the OHP is less than a critical diameter,  $d_b$ , which corresponds to the case when the liquid starts to bridge the flow channel. The critical diameter is determined using the following relation<sup>1,5</sup>.

$$Bo = 2, \quad (1)$$

where the Bond number,  $Bo$ , is expressed as

$$Bo = d_b \sqrt{\frac{g(\rho_l - \rho_g)}{\sigma}}. \quad (2)$$

The co-current two-phase flow dominates in case the vapor superficial velocity is greater than a critical value,  $j_{g,c}$ , so that the vapor can drag the liquid along with it. The vapor superficial velocity is calculated by

$$j_g = \frac{Q}{(n+1)h_{fg}\rho_g A_i}. \quad (3)$$

The critical vapor superficial velocity in the case of vertical operation depends on the following equation<sup>6</sup>.

$$j_g^* = 0.89, \quad (4)$$

where the dimensionless vapor superficial velocity,  $j_g^*$ , is given by

$$j_g^* = \frac{j_{g,c}\rho_g^{0.5}}{[gd_i(\rho_l - \rho_g)]^{0.5}}. \quad (5)$$

Under the assumption that the vapor and liquid are in the saturated state and the heat rates transported by every channel are the same, the minimum heat rate,  $Q_e$ , required to generate the

critical vapor superficial velocity is determined as follows.

$$Q_e = (n+1)h_{fg}A_i\rho_g j_{g,e} . \quad (6)$$

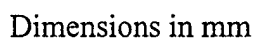
To maintain the proper two-phase flow pattern (the slug flow or co-current two-phase flow), either the condition of  $d_i < d_b$  or  $Q > Q_e$  should be satisfied. A smaller  $Q_e$  is beneficial to the OHP startup.

The passive oscillation movement of the two-phase flow requires that the tubing array of the OHP should have sufficient turns. The minimum tubing turn number for the excited oscillation depends on dynamic balances of mass, momentum, and energy of the two-phase flow in the OHP and heating and cooling boundary conditions. Since constitutive relations of the two-phase flow and heat transfer in the OHP have not been developed, it is difficult to estimate the minimum tubing turn number through numerical simulation. In the present experiment, the tubing turn number of  $n = 40$  is selected according to the present application to the cooling of aircraft EMAs.

There exists the minimum fill ratio of the working fluid in which the OHP can not operate even at a low heat rate, e.g., 10% of its maximum performance. The fill ratio refers to the ratio of the fill liquid volume (at 25°C) to the OHP internal volume. The proper operation of the OHP requires also that the actual fill ratio should be greater than the minimum value,  $\phi > \phi_{\min}$ . Beyond  $\phi_{\min}$ , an increase in  $\phi$  can result in an increase in the internal thermal resistance of the OHP. Concerning this, a proper fill ratio is searched in the present experimental study of the OHP.

### 3 EXPERIMENTAL SETUP AND PROCEDURE

The OHP for the thermal performance test is shown in Figure 3.1. The OHP is made of an 18.61 m long continuous copper tubing with an inner diameter of 1.75 mm and outer diameter of 3.18 mm. The inner radius of the OHP tubing turn is 6.35 mm. The tubing is bent into a multitube planar array having 40 turns, a length of 446 mm and width of 256 mm. Both ends of the tubing are separately sealed. There are two condensers on the looped-ends of the OHP and one evaporator in the middle of the OHP. Lengths of the evaporator, condenser (on either side) and adiabatic section (on either side) are 125 mm, 108.7 mm and 51.8 mm respectively. A photographic view of the OHP connected to a working fluid filling device is shown in Figure 3.2. Acetone, FC-72 and FC-75 are employed as the OHP working fluid. The fluorocarbon fluids of FC-72 and FC-75 are used due to their non-flammability feature. The thermal performance of the fluorocarbon OHPs is compared with that of the acetone OHP. The fill ratio is varied from 32% to 50% for the fluorocarbon fluids and from 25% to 50% for acetone. In the range of the present OHP operating temperature from 25°C to 85°C, the smallest critical tubing inner diameter,  $d_b$ , and the greatest onset heat rate for the co-current two-phase flow,  $Q_e$ , occur at 85°C. For FC-72 and FC-75, the values of  $d_b$  at 85°C are 1.1 mm and 1.38 mm which are smaller than the actual inner diameter of the OHP,  $d_i$  (1.75 mm). However, the values of  $Q_e$  are only 190 W for FC-72 and 110 W for FC-75, small enough to operate the OHP under the condition of the oscillating co-current two-phase flow. For acetone, the value of  $d_b$  at 85°C is 3.0 mm which is greater than the actual inner diameter of the OHP so that the slug flow could exist in the OHP.

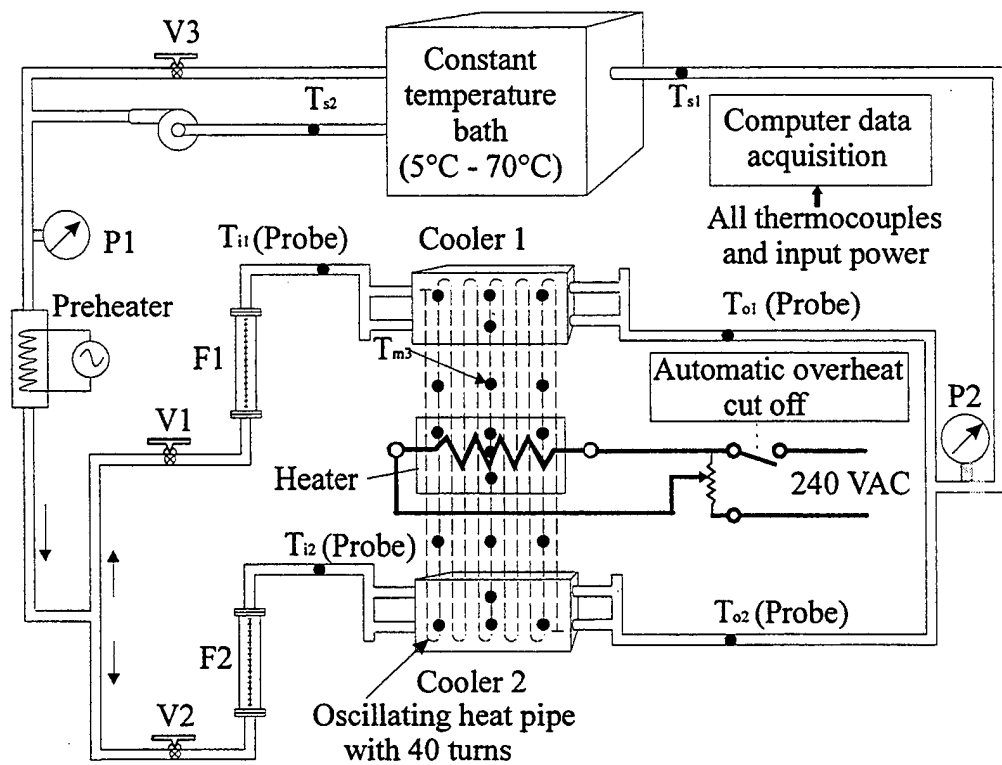


The image shows a document page, likely a ledger or form, with a large, dark, irregular shape in the center. The page is heavily degraded with noise and artifacts. The central shape has some faint markings, including the number '1' and a small cross-like symbol. The page is framed by a dark border.

6



The schematic of OHP experimental setup is shown in Figure 3.3. A drawing of the OHP test hardware including an OHP, a heater assembly and two coolers is presented in Appendix A. The heater contains four aluminum thermal conduction plates, two on one side and the other two on the opposite side of the tube array, covering the evaporator section. The thermal conduction plates are machined, on their contact side with the OHP tube array, into semicircle grooves having the same radius as the OHP tube, as shown in Figure 3.4. The thermal conduction plates are tightly mounted onto the evaporator of the OHP by mechanical joining, as shown in Figure 3.2. To keep a good contact with the OHP tube, thermal conduction grease is applied between the OHP tube and thermal conduction plate. Two electric resistors are installed in the thermal conduction plates, one on each side of the evaporator, and are connected in parallel. There are two coolers, each connecting with one OHP condenser. The main parts of the cooler are a rectangular tank, a couple of rectangular flanges, a couple of sealing bars, RTV sealing material and coolant inlet and outlet manifolds. Water is used as the coolant. In addition to the coolers, the coolant circulation system includes two control valves, one bypass valve, two flowmeters (rotameter type, 0.00631 L/s - 0.0631 L/s), two pressure gauges (0 - 1.03 bar), one preheater, one water pump, one constant temperature bath which contains a filter. The coolant flow rate is controlled by the two control valves. The supply pressure (P1) can be adjusted using bypass valve, V3. The temperature of the coolant bath can be set in the range of 5°C - 70°C. AC power is supplied to the resistance heater through a variac with which the input heat rate can be adjusted. The input power is digitally displayed and recorded by using a MAGTROL power analyzer.



P1, P2 = Pressure gauges    V1, V2 = Flow control valves  
 F1, F2 = Flow meters    V3 = Bypass valve    ● = Thermocouples

Figure 3.3 Schematic of OHP experimental setup.



Nineteen thermocouples of type T with a diameter of 0.2 mm are placed on the OHP wall among which five are located in the evaporator, six in the adiabatic sections and eight in the condensers, as shown in Figure 3.1. The thermocouples can be divided into three groups designated as left group, middle group and right group. The middle group is related with the middle tube, the left group with the 8th tube counted from the left side and the right group with the 8th tube counted from the right side. For each group, the thermocouple locations are indicated in Figure 3.1. In the cooling system, four probe thermocouples,  $T_{i1}$ ,  $T_{i2}$ ,  $T_{o1}$  and  $T_{o2}$  are used to measure the inlet and outlet temperatures of the coolers. Two thermocouples,  $T_{s1}$  and  $T_{s2}$ , are used to monitor the inlet and outlet temperatures of the coolant bath. The signals of the 19 thermocouples are acquired using a KEITHLEY 500A measurement and control unit supported by a Viewdac data acquisition and control program. In addition, 38 thermocouples are attached to the rest of the tubes at locations close to the top of the evaporator to monitor the temperature of each tube. These thermocouples are connected to a rotary switch from which a thermocouple is led to a FLUKE 2100A digital thermometer. For the safe operation, a thermocouple measuring the evaporator temperature is connected to a high temperature cut out unit. If the temperature is too high, the power supply will automatically cut out.

The tests are started by turning on the coolant circulation system, setting flow rate, and controlling the supply pressure (P1) by adjusting the bypass valve. The variac is then adjusted until a desired electric power is displayed on the MAGTROL unit. The OHP operating temperature (temperature level) indicated by the temperature of  $T_{m3}$  is maintained to be a constant by adjusting the flow rate and coolant bath temperature for different input powers. After the system attains steady state, the temperature, flow rate and input power are recorded. The present experiment conditions are as follows:

OHP temperature level:	25°C - 85°C with 10°C intervals.
Input power:	140 W - 2100 W.
Coolant flow rate:	0.00631 L/s - 0.025 L/s for each flowmeter.
Coolant inlet temperature:	2.4°C - 68.2°C.
Fluid fill ratio:	50% (22.5 ml), 38% (16.9 ml), 32% (14.24 ml), 25% (11.1 ml).
OHP orientation:	Vertical (indicated in Figure 3.1)

and horizontal (with the multitube array in the horizontal plane).

The inlet temperature of the coolant for the top cooler is almost the same as that for the bottom cooler. During the experiment, the flow rates through the top flowmeter and bottom flowmeter are set to be the same.

#### 4 MEASUREMENT UNCERTAINTY

The data acquisition unit and thermocouples are compared to a precision digital resistance temperature device (RTD), with  $0.03^{\circ}\text{C}$  rated accuracy, over the range of interest. The temperature measurement system accuracy values for the 0.2 mm thermocouples (on the OHP wall) and for the four thermocouples of probe type are  $0.2^{\circ}\text{C}$  and  $0.1^{\circ}\text{C}$  respectively. The accuracy of the thermocouple locations in reference to the top of OHP is 2.0 mm. The flowmeters are calibrated using a measuring glass and stopwatch at temperatures of  $10^{\circ}\text{C}$ ,  $25^{\circ}\text{C}$ ,  $40^{\circ}\text{C}$ ,  $50^{\circ}\text{C}$  and  $60^{\circ}\text{C}$ . The accuracy of calibrated flow rate is within  $3.2 \times 10^{-4}$  L/s. The calibration result shows that the coolant temperature has negligible influence on the flow rate greater than 0.0095 L/s. The uncertainty of the electrical power input through the power analyzer is 0.5% of reading.

Heat losses are less than 25% of the input power at input powers greater than 500 W. The heat loss results from the temperature difference between the OHP and environment. Overall uncertainties for the heat transfer coefficients of evaporator and condenser are estimated and plotted along with the corresponding data in resultant figures presented in this report.

## 5 RESULTS AND DISCUSSION

To estimate the heat transfer characteristics of the OHP, mean temperature differences are calculated as follows:

$$\Delta T_{e1} = T_e - T_{a1}, \quad (7)$$

$$\Delta T_{e2} = T_e - T_{a2}, \quad (8)$$

$$\Delta T_{c1} = T_{a1} - T_{c1}, \quad (9)$$

$$\Delta T_{c2} = T_{a2} - T_{c2}, \quad (10)$$

where  $T_e$  is the mean temperature of the 5 thermocouples in the evaporator,  $T_{a1}$  and  $T_{a2}$  are the mean temperatures of the 3 thermocouples in the upper adiabatic section and those in the lower adiabatic section,  $T_{c1}$  and  $T_{c2}$  are the mean temperatures of the 4 thermocouples in the upper condenser and those in the lower condenser. The heat transfer coefficients with respect to the evaporator and condensers are defined as follows:

$$h_{e1} = \frac{Q_1}{A_e \Delta T_{e1}}, \quad (11)$$

$$h_{e2} = \frac{Q_2}{A_e \Delta T_{e2}}, \quad (12)$$

$$h_{c1} = \frac{Q_1}{A_{c1} \Delta T_{c1}}, \quad (13)$$

$$h_{c2} = \frac{Q_2}{A_{c2} \Delta T_{c2}}, \quad (14)$$

where  $A_e$  is the outer area of the total tubes in the evaporator,  $A_{c1}$  the outer area of the total tubes in the upper condenser,  $A_{c2}$  the outer area of the total tubes in the bottom condenser,  $Q_1$  the heat rate through the upper condenser, and  $Q_2$  the heat rate through the lower condenser.

### 5.1 Results of Acetone Heat Pipe

During the thermal performance experiment for acetone OHP under the present experimental conditions, no dryout on any tube wall of the evaporator has been found at input power rates up to

2100 W. This means that the performance of the OHP is excellent.

Figure 5.1 shows a comparison between the heat rate through the upper condenser and lower condenser at the operating temperature of 55°C for the fill ratios of 50% and 38%. In horizontal operation, the heat rate through the upper condenser is approximately equal to that through the lower condenser. In vertical operation, the heat rate through the upper condenser is higher than that through the lower condenser but the difference becomes negligibly small at total heat rates,  $Q = Q_1 + Q_2$ , greater than 700 W.

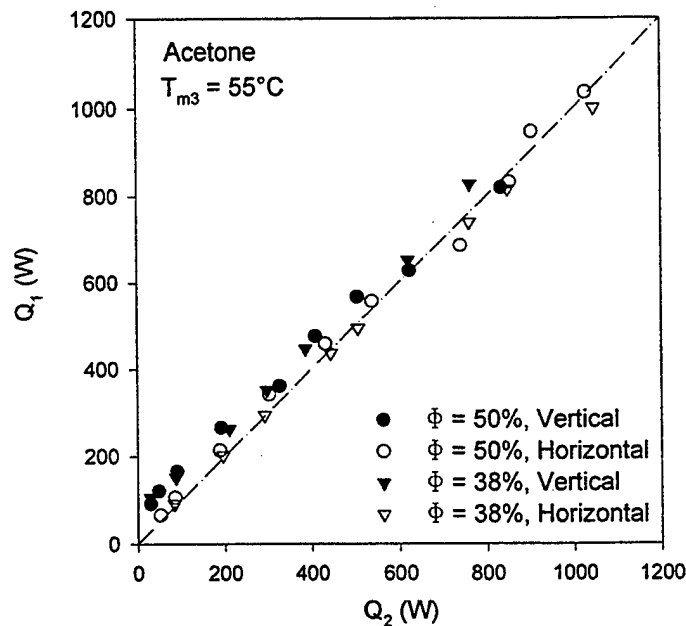


Figure 5.1 Comparison between the heat rate through the upper condenser ( $Q_1$ ) and lower condenser ( $Q_2$ ).

Figure 5.2 and Figure 5.3 show the heat transfer coefficients of the evaporator and condenser vs. the total heat rate for  $T_{m3} = 55^\circ\text{C}$  and  $\phi=50\%$  in vertical and horizontal operations. As shown in Figure 5.2, the heat transfer coefficients increase with the heat rate up to 880 W, and then vary only slightly with the heat rate in the high heat rate region. The increase of the heat rate results in an increase of the vapor and liquid velocities in the OHP and intensifies the flow boiling heat transfer and condensation heat transfer. On the other side, the increase of the flow velocities brings about a



rise of the flow pressure drop and consequently enlarges the mean temperature differences expressed in equations (7) through (10). In the present case, the former trend is dominant at the heat rates up to 880 W. It can be seen from Figure 5.2 and Figure 5.3 that the heat transfer coefficient of  $h_{e1}$  is greater than that of  $h_{e2}$ , and  $h_{c1}$  is greater than  $h_{c2}$  at heat rates less than 700 W. The difference becomes small at heat rates higher than 700 W. In Figure 5.3, the heat transfer coefficients increase with the heat rate up to 640 W, and then change only slightly with the heat rate except at the heat rate of 1430 W where relatively low heat transfer coefficients occur. The heat transfer coefficients of the evaporator and condenser in the high heat rate region are slightly greater than those as shown in Figure 5.2.

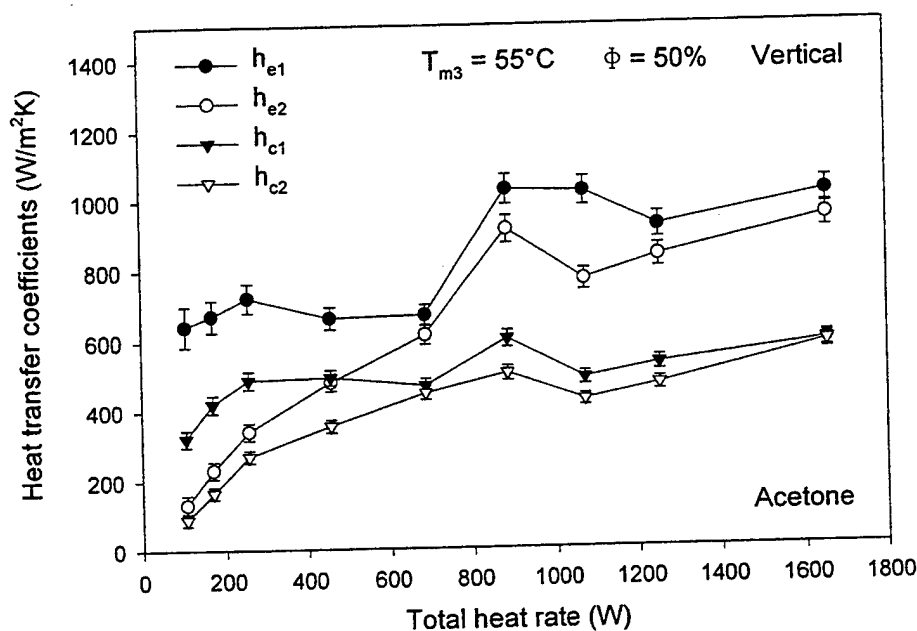


Figure 5.2 Heat transfer coefficients vs. total heat rate for  $T_{m3} = 55^\circ\text{C}$  and  $\phi = 50\%$  in vertical position.

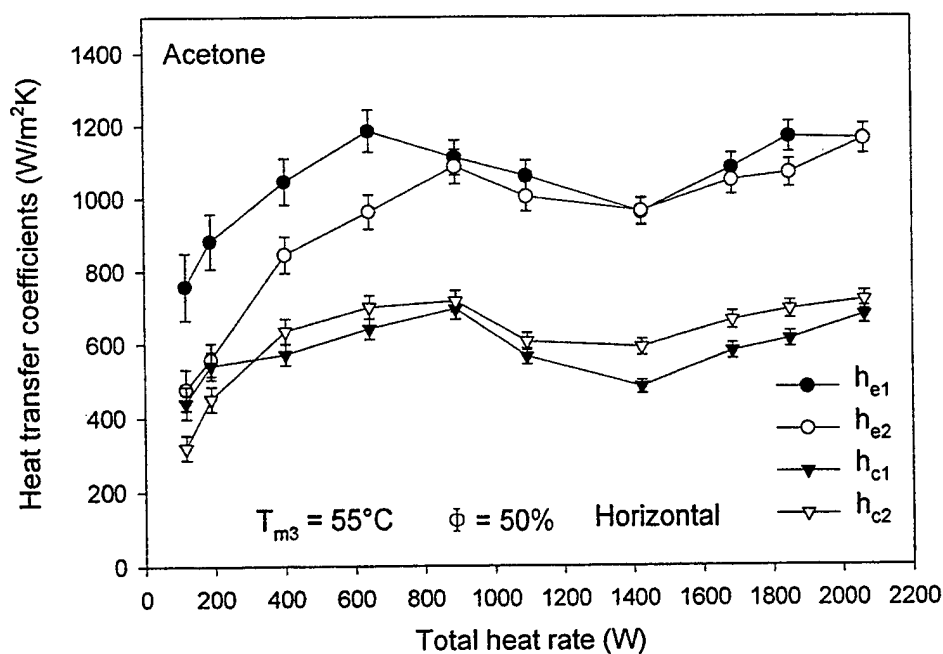


Figure 5.3 Heat transfer coefficients vs. total heat rate for  $T_{m3} = 55^\circ C$  and  $\phi = 50\%$  in horizontal position.

Figure 5.4 shows a comparison of the heat transfer coefficients of the evaporator and condenser between the case of  $\phi = 38\%$  and  $\phi = 50\%$  at  $T_{m3} = 55^\circ C$  in the vertical operation. For  $\phi = 38\%$ , the heat transfer coefficients of the evaporator and condenser increase with the heat rate up to 470 W and then change only slightly with the heat rate. At the heat rates greater than 230 W, the heat transfer coefficients of the evaporator and condenser are greater for  $\phi = 38\%$  than for  $\phi = 50\%$ .

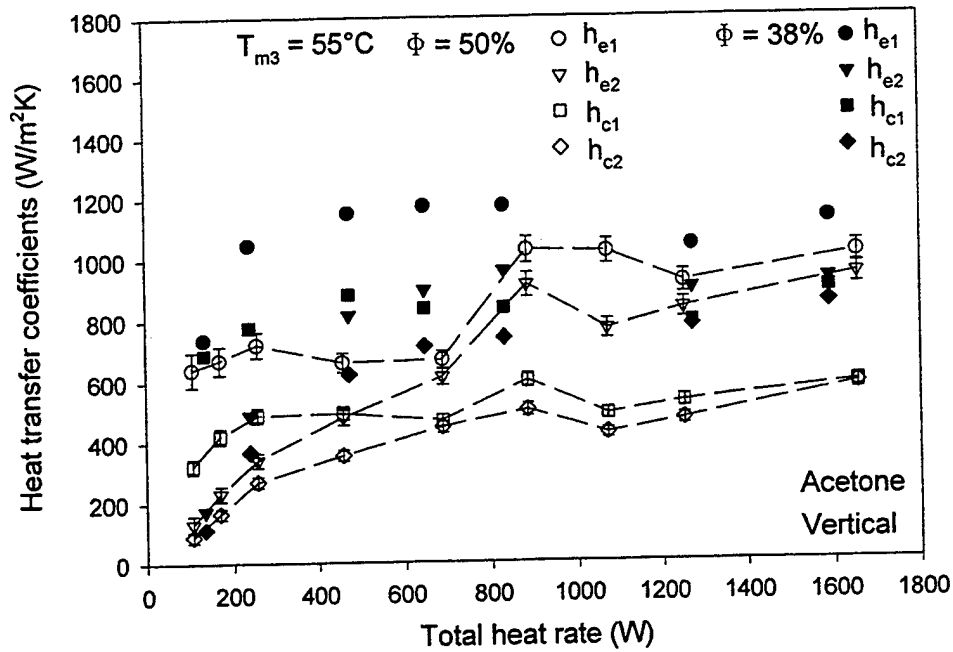


Figure 5.4 Heat transfer coefficients vs. total heat rate for  $\phi=50\%$  and  $\phi=38\%$  at  $T_{m3} = 55^\circ\text{C}$  in vertical position.

Figure 5.5 and Figure 5.6 show OHP wall temperature profiles along the middle tube in vertical operation at  $T_{m3}=55^\circ\text{C}$  for  $\phi=38\%$  and  $\phi=32\%$ . In Figure 5.5, the wall temperature generally increases with an increase of the distance up to the evaporator section and then decreases. There are three thermocouples in the evaporator, two in the upper condenser, one in the upper adiabatic section, one in the lower adiabatic section and two in the lower condenser. The thermocouple indicating the highest temperature is located in the middle part of the evaporator due to a higher heat flux in the middle. The higher the heat rate, the larger the temperature difference is between the evaporator and condenser. The average temperature difference between the evaporator and condensers is  $33^\circ\text{C}$  at  $1590\text{ W}$ . The variation of the wall temperature in Figure 5.6 is close to that in Figure 5.5 and the average temperature difference between the evaporator and condensers is  $35^\circ\text{C}$  at  $1670\text{ W}$ .

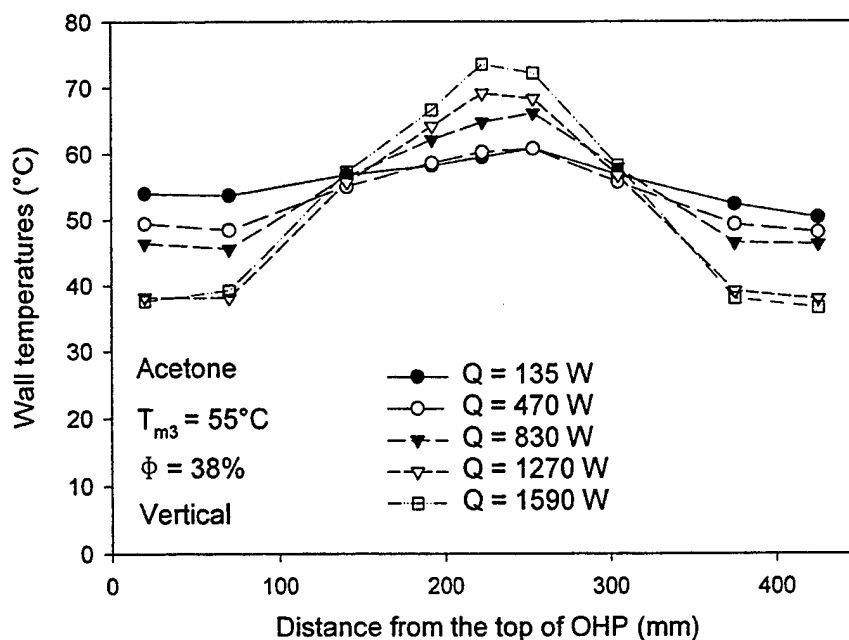


Figure 5.5 OHP wall temperature profiles along the middle tube of the OHP at different total heat rates for  $T_{m3} = 55^{\circ}\text{C}$  and  $\phi = 38\%$  in vertical operation.

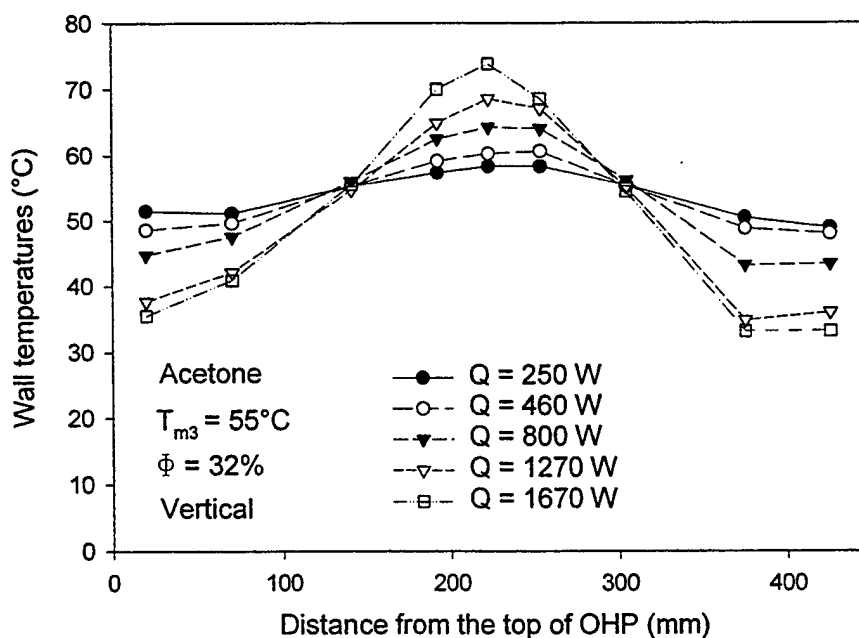


Figure 5.6 OHP wall temperature profiles along the middle tube of the OHP at different total heat rates for  $T_{m3} = 55^{\circ}\text{C}$  and  $\phi = 32\%$  in vertical operation.

Figure 5.7 shows the heat transfer coefficients of the upper evaporator and condenser vs. the operating temperature at heat rates in a narrow range of 780 W to 880 W in vertical operation. It seems that the heat transfer coefficients vary only slightly with the operating temperature. The heat transfer coefficients for  $\phi=38\%$  are close to those for  $\phi=32\%$ . The heat transfer coefficients for  $\phi=38\%$  and  $\phi=32\%$  are higher than those for  $\phi=50\%$ .

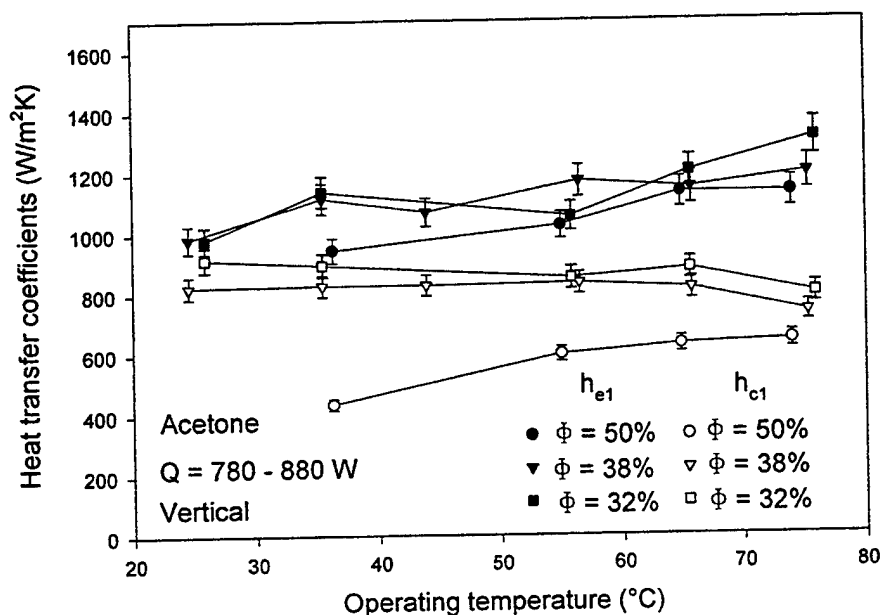


Figure 5.7 Heat transfer coefficients of the upper evaporator and condenser vs. operating temperature.

## 5.2 Results of Fluorocarbon Heat Pipes

For the FC-72 OHP with the fill ratio of 50% vertically operating at a temperature level of 75°C and 85°C ( $T_{m3}$ ), no dryout on any tube wall of the evaporator has been found at total heat rates up to 2040 W. However, the fluorocarbon OHPs with the 32% fill ratio can not operate appropriately even at the low input power of 200 W due to the occurrence of the dryout in the evaporator.

Figure 5.8 shows wall temperature profiles of the FC-72 OHP along the middle tube in vertical operation for  $T_{m3}=75^\circ\text{C}$  and  $\phi=50\%$  at different total heat rates. Generally, the wall temperature increases with an increase of the distance up to the evaporator section and then decreases. There are three thermocouples in the evaporator, two in the upper condenser, one in the upper adiabatic section, one in the lower adiabatic section and two in the lower condenser. The thermocouple indicating the highest temperature is located in the middle part of the evaporator. The higher the heat rate, the larger the temperature difference is between the evaporator and condenser. The average temperature difference between the evaporator and condensers is 46°C at 2040 W. No temperature excursion has been found at the achievable heat rates up to 2040 W.

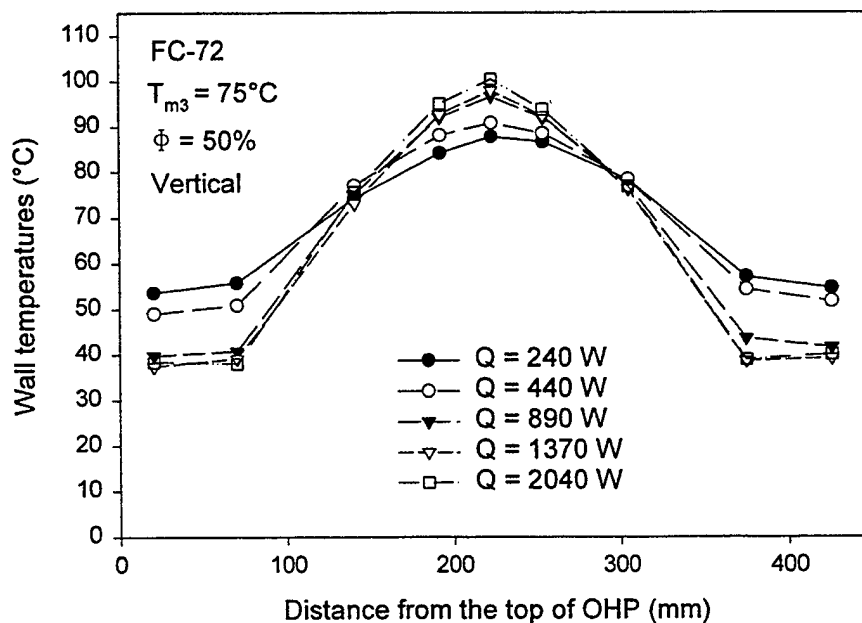


Figure 5.8 OHP wall temperature profiles along the middle tube of the FC-72 OHP at different total heat rates for  $T_{m3} = 75^\circ\text{C}$  and  $\phi=50\%$  in vertical operation.

Figure 5.9 gives heat transfer coefficients of the evaporator and condenser as a function of the heat rate for the FC-72 OHP in vertical and horizontal operations for  $T_{m3}=75^{\circ}\text{C}$  and  $\phi=50\%$ . The heat transfer coefficients increase with the heat rate. The differences between  $h_{e1}$  and  $h_{e2}$  and between  $h_{c1}$  and  $h_{c2}$  are not significant in vertical operation or horizontal operation. The difference between the results for the vertical operation and those for the horizontal operation is small.

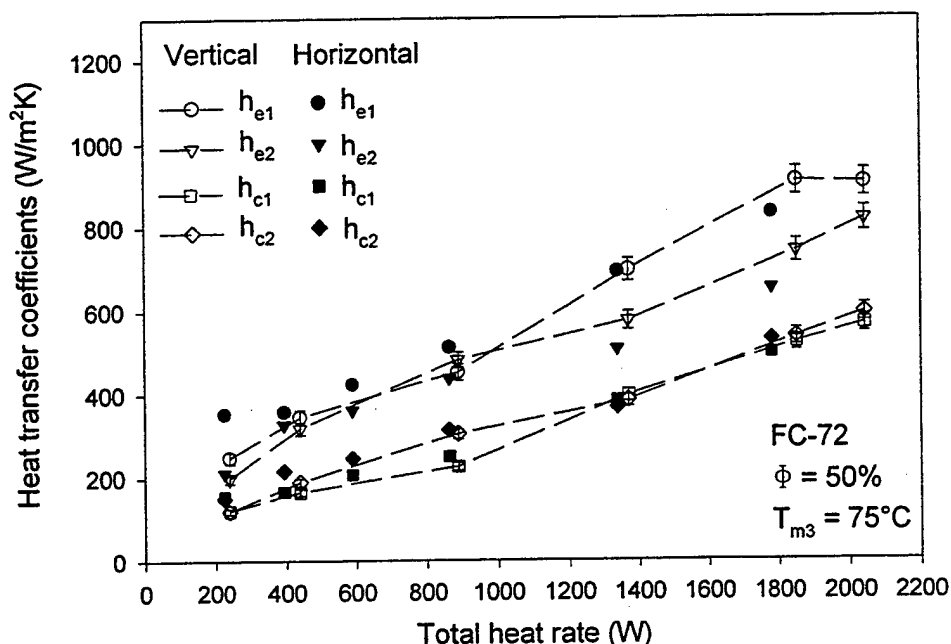


Figure 5.9 Heat transfer coefficients of the evaporator and condenser vs. total heat rate for FC-72 OHP with 50% fill ratio at  $75^{\circ}\text{C}$  operating temperature.

Figure 5.10 shows heat transfer coefficients of the evaporator and condenser as a function of the heat rate for the FC-75 OHPs with the 50% and 38% fill ratios in vertical operation at the operating temperature of  $75^{\circ}\text{C}$ . The heat transfer coefficients increase with the heat rate. The OHP with the 38% fill ratio has undergone the dryout at input heat rates of 800 W. The heat transfer coefficients of the evaporator are slightly lower with the 38% fill ratio than those with the 50% due to insufficient wetting of the evaporator wall. The difference of the heat transfer coefficients of the condenser between  $\phi=38\%$  and  $\phi=50\%$  is small. An excursion of temperatures on the OHP with the

38% fill ratio during the dryout is shown in Figure 5.11. At the total heat rate of 700 W, the OHP operates appropriately in the steady state. At the total heat rate of 800 W, the temperature in the evaporator,  $T_{m5}$ , starts to continuously increase and the temperature in the upper condenser begins to drop. The operation of the OHP is deteriorated due to the dryout in the evaporator.

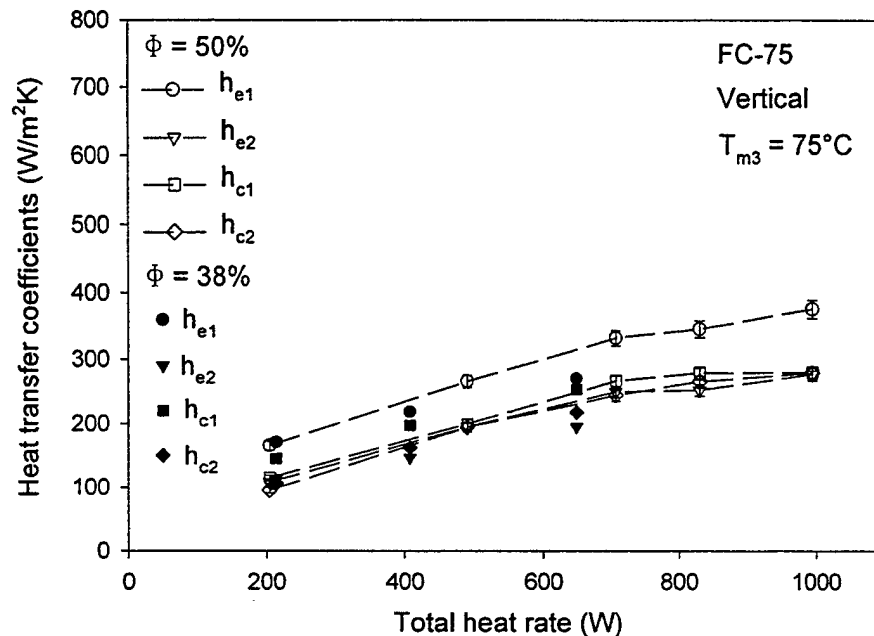


Figure 5.10 Heat transfer coefficients of the evaporator and condenser vs. total heat rate for FC-75 OHP in vertical operation at  $75^\circ C$  operating temperature.



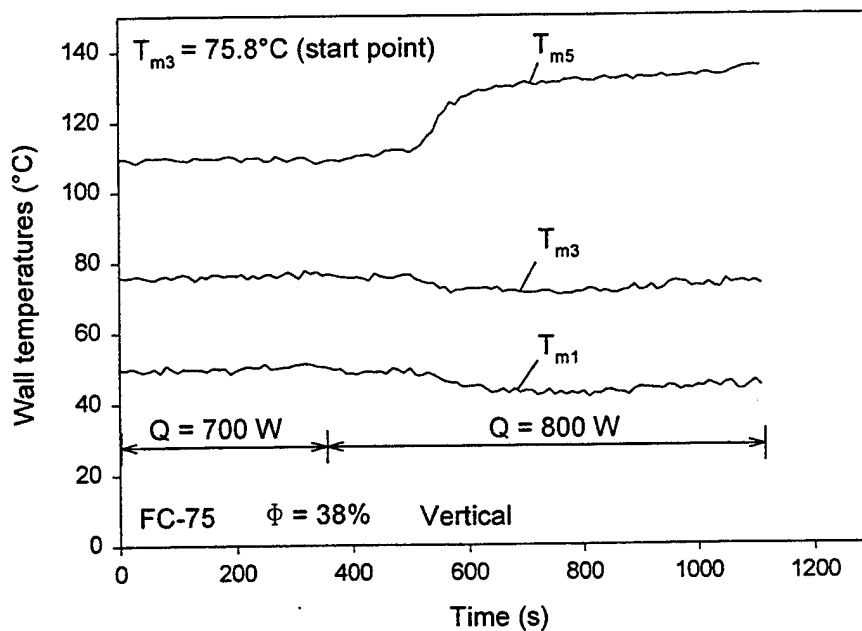


Figure 5.11 Excursion of temperatures on the FC-75 OHP with 38% fill ratio during dryout.

Figure 5.12 shows heat transfer coefficients of the upper evaporator and condenser vs. the operating temperature for the FC-72 OHP with the 50% fill ratio in vertical operation at heat rates of 455 W and 1390 W. The heat transfer coefficient of the upper condenser decreases only slightly with the operating temperature. The heat transfer coefficient of the upper evaporator increases with the operating temperature up to 75°C for  $Q = 1390 \text{ W}$  and up to 55°C for  $Q = 455 \text{ W}$ . The heat transfer coefficients of the upper evaporator and condenser are much higher for  $Q = 1390 \text{ W}$  than those for  $Q = 455 \text{ W}$ .

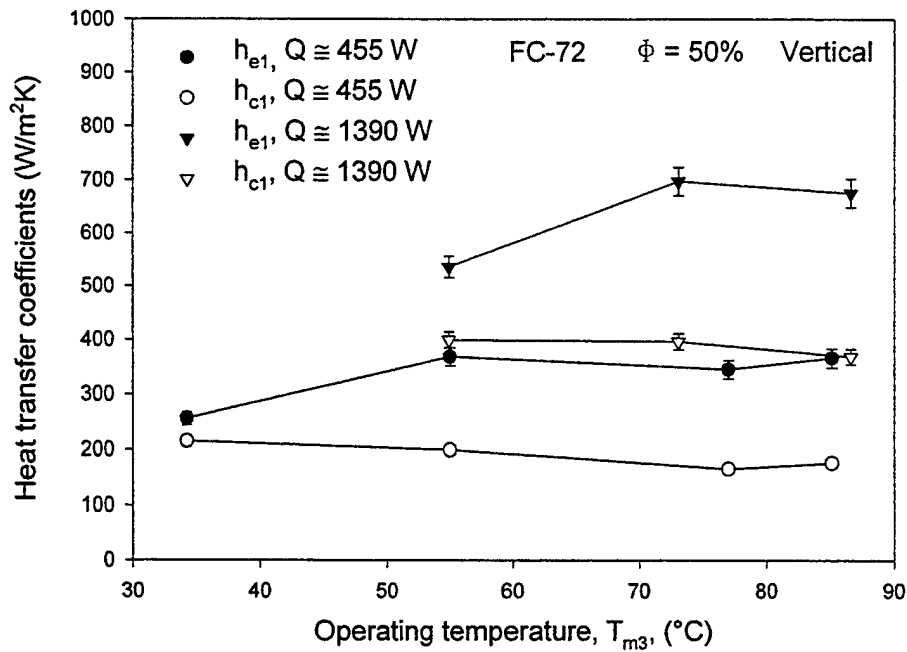


Figure 5.12 Heat transfer coefficients of the upper evaporator and condenser vs. operating temperature.

Figure 5.13 shows a comparison between the heat rate through the upper condenser and lower condenser of the FC-72 and FC-75 OHPs with the fill ratio of 50% at various operating temperatures. The heat rate transferred through the upper condenser is approximately the same as through the lower condenser in both vertical and horizontal operations. Figure 5.14 shows the comparison of the heat transfer coefficients of the upper evaporator and condenser in vertical position with those in horizontal position for the fluorocarbon OHPs with the 50% and 38% fill ratios at heat rates between 175 W and 1850 W and at operating temperatures between 25°C and 75°C. The result indicates that there is no significant difference between the heat transfer coefficients of evaporator and condenser in the horizontal position and those in the vertical position. The result implies that the thermal performance of the OHPs is insensitive to the gravitational acceleration. The heat transfer coefficients vary widely, from 134 W/m<sup>2</sup>K to 907 W/m<sup>2</sup>K for  $h_{e1}$  and from 66 W/m<sup>2</sup>K to 520 W/m<sup>2</sup>K for  $h_{c1}$ , depending on the working fluid and operating condition.

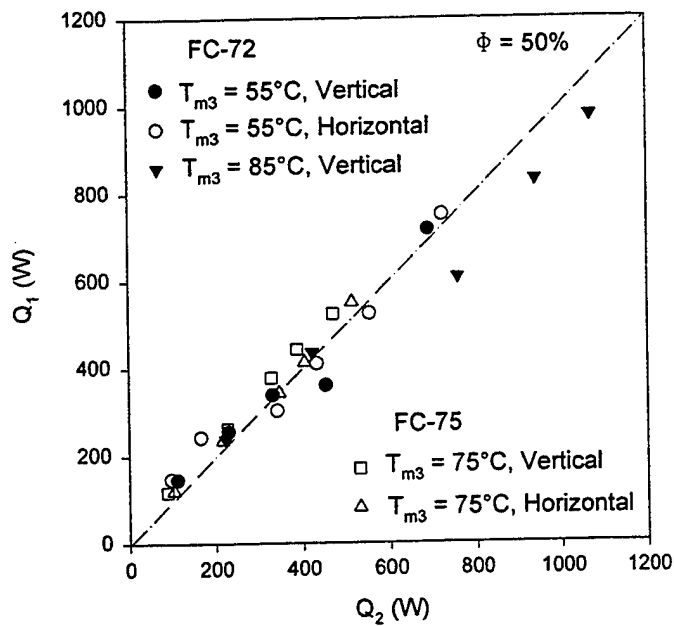


Figure 5.13 Comparison between the heat rate through the upper condenser ( $Q_1$ ) and lower condenser ( $Q_2$ ) of the FC-72 and FC-75 OHPs.

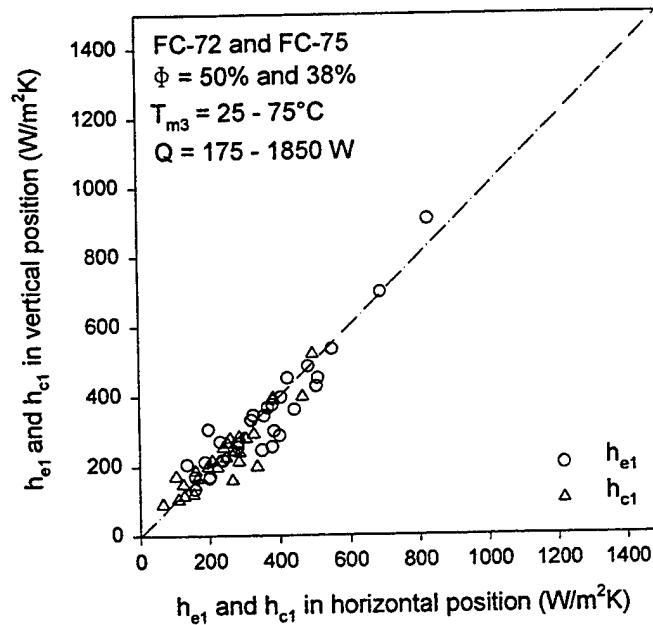


Figure 5.14 Comparison of the heat transfer coefficients of the upper evaporator and condenser in vertical position with those in horizontal position.

### 5.3 Comparison of OHPs With Different Working Fluids

It can be seen from Figure 5.5 and Figure 5.8 that the average temperature difference between the evaporator and condenser is significantly larger for FC-72 OHP than for acetone OHP. Figure 5.15 shows the comparison of heat transfer coefficients of the acetone OHP with those of the FC-72 OHP and FC-75 OHP with respect to the upper evaporator and condenser. The OHPs have the fill ratio of 50% and operate horizontally at  $T_{m3}=75^{\circ}\text{C}$ . The heat transfer coefficients of evaporator of the FC-72 OHP are lower than those of the acetone OHP while higher than those of the FC-75 OHP. The heat transfer coefficients of condenser of the FC-72 OHP are lower than those of the acetone OHP while approximately the same as the FC-75 OHP. The difference of the heat transfer coefficients of evaporator as well as the condenser between the acetone OHP and FC-72 OHP becomes smaller with increasing the heat rate.

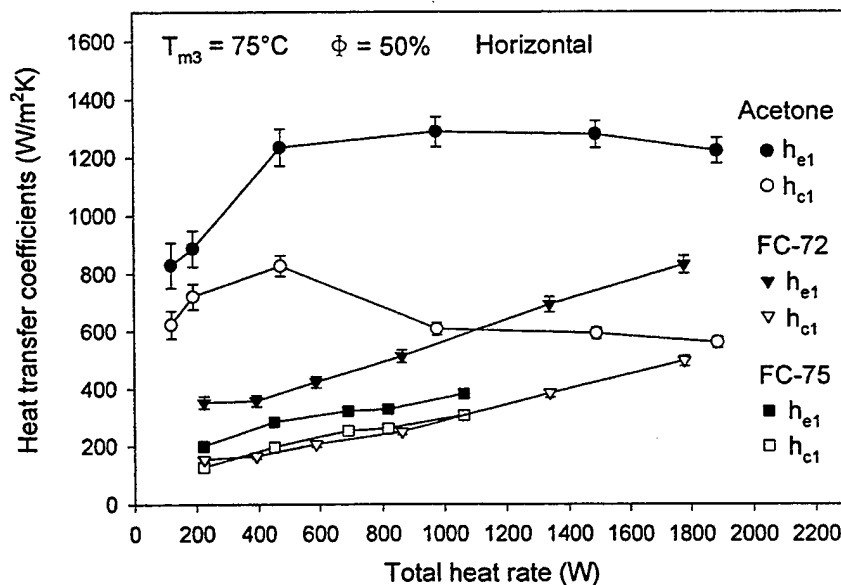


Figure 5.15 Comparison of heat transfer coefficients of the FC-72 OHP with those of FC-75 OHP and acetone OHP with respect to the upper evaporator and condenser.

## 6 CONCLUSIONS AND RECOMMENDATIONS

### 6.1 Conclusions

1. The acetone OHP with the fill ratios of 50%, 38% and 32% and the FC-72 OHP with the fill ratio of 50% have the capability of transporting more than 2040 W without dryout.
2. The performance limitation of the fluorocarbon OHPs is caused by the dryout which is indicated by the excursion of the temperatures on the OHP wall. The dryout limit of the fluorocarbon OHPs is much higher for the 50% fill ratio than for the 38%. This means that the fill ratio of 38% is not sufficient for the fluorocarbon OHPs. The fluorocarbon OHPs can not operate in the case of the 32% fill ratio even at the low input power of 200 W. The acetone OHP does not operate appropriately for the fill ratio of 25%.
3. For the acetone OHP, the heat transfer coefficients of the evaporator and condenser are noticeably higher for the fill ratios of 38% and 32% than those for 50%. The desired fill ratio is 38%.
4. In most cases, the heat transfer coefficients of the fluorocarbon OHPs increase with the heat rate. In most cases, the heat transfer coefficients of the acetone OHP increase with the heat rate up to a heat rate between 470 W and 900 W and then change only slightly with the heat rate.
5. The heat rate dissipated through the upper condenser is approximately the same as through the lower condenser (in both vertical and horizontal operations). The energy transport of the OHP is attributed to the excited oscillation of the two-phase flow in the OHP. The tubing turn number of 40 used in the present experiment is sufficiently large to generate the oscillation in the OHP.
6. There is no significant difference between the heat transfer coefficients of evaporator and condenser of the fluorocarbon OHPs in the horizontal position and those in the vertical position.
7. At a same operating temperature, the heat transfer coefficients of evaporator of the FC-72 OHP are lower than those of the acetone OHP while higher than those of the FC-75 OHP. The heat transfer coefficients of condenser of the FC-72 OHP are lower than those of the acetone OHP while approximately the same as the FC-75 OHP. The difference of the heat transfer coefficients of evaporator as well as the condenser between the acetone OHP and FC-72 OHP becomes smaller with increasing the heat rate.

## 6.2 Recommendations

The following recommendations are made to expand the OHP research.

- ◆ OHP thermal performance tests at temperatures higher than 85°C may be required for the fluorocarbon fluids or organic fluids.
- ◆ The influence of g-load on the OHP thermal performance needs to be investigated for aircraft application. The thermal performance test under g-load can be conducted using a spin table.
- ◆ An effective operation of the OHP requires that the tubing array of the OHP should have sufficient turns. This requirement implies that there might exist the minimum number of the tubing turns. To determine the minimum tubing turn number, more experimental investigations under various operating conditions should be carried out using several different tubing turns. Meanwhile, a theoretical modeling of the minimum tubing turn number may be carried out based on governing equations of the two-phase flow in the OHP and heating and cooling boundary conditions. Necessary constitutive relations of the two-phase flow and heat transfer in the OHP need to be developed.

## 7 REFERENCES

<sup>1</sup>Maezawa, S., Gi, K., Minamisawa, A., and Akachi, H., "Thermal Performance of Capillary Tube Thermosyphon," 9th Int. Heat Pipe conference, Albuquerque, 1995.

<sup>2</sup>Maezawa, S., Nakajima, R., Gi, K., and Akachi, H., "Experimental Study on Chaotic Behavior of Thermohydraulic Oscillation in Oscillating Thermosyphon," 5th Int. Heat Pipe Symposium, Melbourne, 1996.

<sup>3</sup>Akachi, H. and Polasek, F., "Thermal Control of IGBT Modules in Traction Drives by Pulsating Heat Pipes," 10th Int. Heat Pipe Conference, Stuttgart, 1997.

<sup>4</sup>Kiseev, V. M. and Zolkin, K. A., "The Influence of Acceleration on The Performance of Oscillating Heat Pipe," 11th Int. Heat Pipe Conference, Tokyo, 1999.

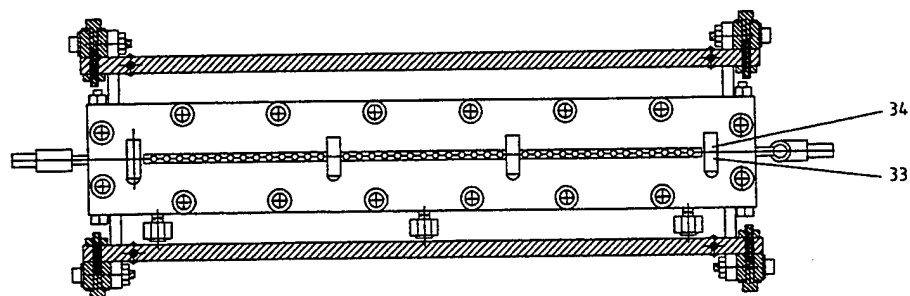
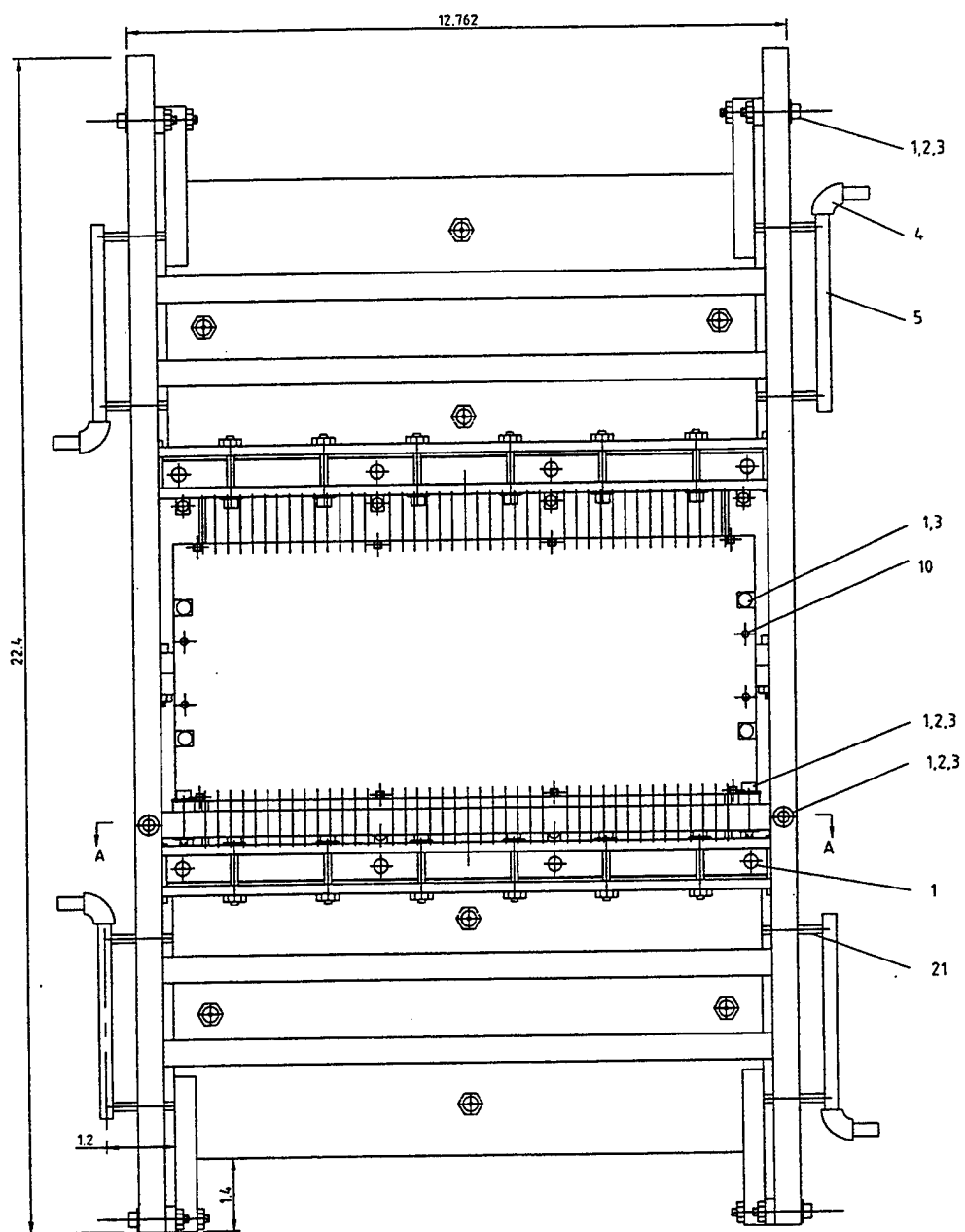
<sup>5</sup>Chen, H., Groll, M., and Roesler, S., "Micro Heat Pipes: Experimental Investigation and Theoretical Modeling," 8th Int. Heat Pipe Conference, Beijing, 1992.

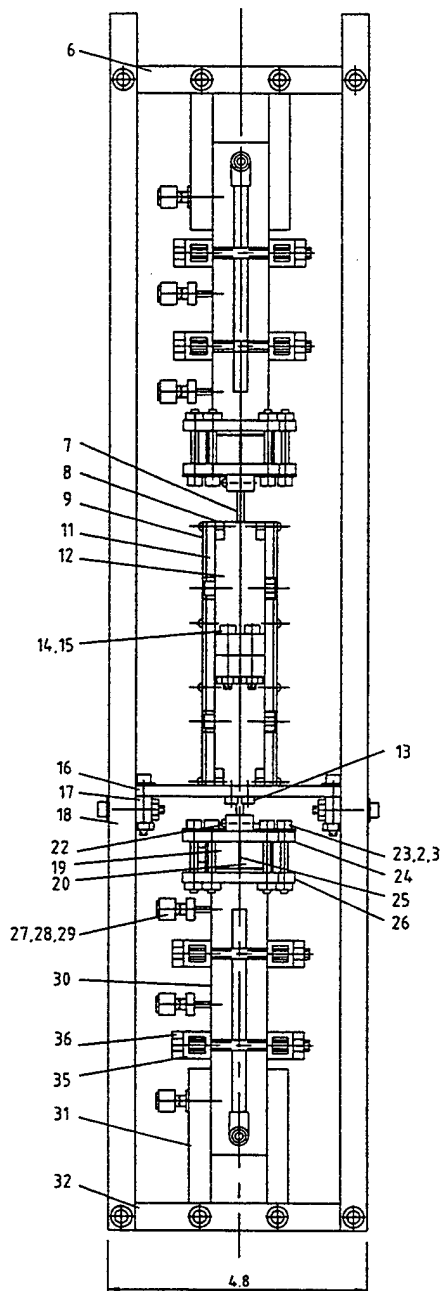
<sup>6</sup>Whalley, P. B., "Boiling, Condensation, and Gas-Liquid Flow," Oxford University Press, New York, 1987, pp. 112-114.

## **APPENDIX A**

### **ASSEMBLY DRAWING OF OHP TEST RIG**







36	8	PUR	#12-24 UNC-2A x 12.3 HEX HD. S. S.
35	8	PUR	SQUARE TUBE 0.5x0.5x12.3
34	8	98001F-17	HOLDER (2), COPPER
33	8	98001F-16	HOLDER (1), COPPER
32	2	98001F-15	HORIZONTAL FRAME, ALUMINUM
31	8	98001F-14	TANK SUPPORT, COPPER
30	2	98001F-13	COOLING TANK, COPPER
29	8	PUR	1 TZ-T 1/16 FERRULE-TEFLON
28	8	PUR	2-1 TRBZ 1/16 TUBE END REDUCER NUT COPPER
27	8	PUR	2-1 TRBZ 1/16 TUBE END REDUCER BODY COPPER
26	2	98001F-12	RECTANGULAR FRANGE, COPPER
25	2	PUR	RTV SEALING
24	4	98001F-11	HALF FRANGE, COPPER
23	32	PUR	#8-32 UNC-2A x 1.25 SOC. HD. CAP SCR. S. S.
22	8	PUR	#4-40 UNC-2A x 1/2 ROUND HD. CAP SCR. S. S.
21	8	PUR	3/16 CONNECTING PIPE, COPPER
20	2	98001F-10	SEALING HALF (2), ALUMINUM
19	2	98001F-09	SEALING HALF (1), ALUMINUM
18	4	98001F-08	VERTICAL FRAME, ALUMINUM
17	2	98001F-07	SUPPORT FRAME, ALUMINUM
16	2	98001F-06	SUPPORT BEAM, ALUMINUM
15	4	PUR	#6x0.109 MACH. SCR. NUT HEX S. S.
14	4	PUR	#6-32 UNC-2A x 1.0 SOC. HD. CAP SCR. S. S.
13	4	PUR	#6-32 UNC-2A x 1/2 SOC. HD. CAP SCR. S. S.
12	4	98001F-05	HEATING BLOCK, ALUMINUM
11	2	PUR	0.1 THICK INSULATION SHEET, CERAMIC PAPER G/I-83
10	16	PUR	#2-56 UNC-2A x 3/8 ROUND HD. CAP SCR. S. S.
9	2	98001F-04	1/16 ALUMINUM SHEET
8	4	98001F-03	INSULATION BEAM, ALUMINUM
7	1	98001F-02	PULSATING HEAT PIPE, COPPER
6	2	98001F-01	HORIZONTAL BEAM, ALUMINUM
5	4	PUR	1/4 COOLANT PIPE
4	4	PUR	1/4 90° TUBE CONNECTOR
3	60	PUR	#8x0.13 MACH. SCR. NUT HEX S. S.
2	56	PUR	#8 FLAT WASHER S. S.
1	36	PUR	#8-32 UNC-2A x 1.0 SOC. HD. CAP. SCR. S. S.
NO.	QUAN.	ITEM	DESCRIPTION

#### PARTS LIST

UNLESS OTHERWISE SPECIFIED

DIMENSIONS ARE IN INCHES - TOLERANCES ON:

FRACTIONS

DECIMALS

ANGLES

± 1/64

.XX ± .01

± 1/2°

.XXX ± .005

UES

Dayton, OHIO 45432-1894

DR. BY - DATE

Lanchao Lin

DES. BY - DATE

Lanchao Lin

CHK. BY - DATE

TITLE

OSCILLATING HEAT PIPE  
TEST RIG

PROJECT

155-002

SIZE  
A3

DRAWING NUMBER  
98001F

SCALE

98001F\_1

SHEET  
1 OF 13